Eur Spine J (1998) 7 : 59–65

Three-dimensional measurement of wedged scoliotic vertebrae and intervertebral disks

C.-E. Aubin
J. Dansereau
Y. Petit
F. Parent
J. A. de Guise
H. Labelle

Received: 4 January 1997
Revised: 26 July 1997
Accepted: 1 August 1997

C.-E. Aubin (✉) · J. Dansereau · Y. Petit
Department of Mechanical Engineering,
École Polytechnique,
P.O. Box 6079, Station "Centre-Ville",
Montréal, Quebec, H3C 3A7, Canada,
and Research Center,
Sainte-Justine Hospital,
Montréal, Québec, Canada
Tel. +1-514-340-4711 ext. 4437;
Fax +1-514-340-5867;
e-mail: aubin@grbb.polymtl.ca

F. Parent
Department of Mechanical Engineering,
École Polytechnique,
Montréal, Québec, Canada

J. A. de Guise
Research Center, Sainte-Justine Hospital,
and Department of
Automated Production Engineering,
École de Technologie Supérieure,
Montréal, Québec, Canada

H. Labelle
Research Center, Sainte-Justine Hospital,
Montréal, Québec, Canada

Abstract Idiopathic scoliosis involves complex spinal intrinsic deformations such as the wedging of vertebral bodies (VB) and intervertebral disks (ID), and it is obvious that the clinical evaluation obtained by the spinal projections on the two-dimensional (2D) radiographic planes do not give a full and accurate interpretation of scoliotic deformities. This paper presents a method that allows reconstruction in 3D of the vertebral body endplates and measurement of the 3D wedging angles. This approach was also used to verify whether 2D radiographic measurements could lead to a biased evaluation of scoliotic spine wedging. The 3D reconstruction of VB contours was done using calibrated biplanar X-rays and an iterative projection computer procedure that fits 3D oriented ellipses of adequate diameters onto the 3D endplate contours. "3D wedging angles" of the VB and ID (representing the maximum angle between adjacent vertebrae) as well as their angular locations with respect to the vertebral frontal planes were computed by finding the positions of the shortest and longest distances between consecutive endplates along their contour. This method was extensively validated using several approaches: (1) by comparing the 3D reconstructed endplates of a cadaveric functional unit (T_8-T_9) with precise 3D measurements obtained using a coordinate measuring machine for 11 different combinations of vertebral angular positions; (2) by a sensitivity study on 400 different vertebral segments mathematically generated, with errors randomly introduced on the digitized points (standard deviations of 0.5, 1, 2, and 3 mm); (3) by comparing the clinical wedging measurements (on postero-anterior and lateral radiographs) at the thoracic apical level of 34 scoliotic patients (15° < Cobb < 45°) to the computed values. Mean errors for the 11 vertebral positions were 0.5 ± 0.4 mm for VB thickness, less than 2.2° for endplate orientation, and about 11° (3 mm) for the location of the maximum 3D wedging angle along the endplate contour. The errors below 2 mm (introduced on the digitized points) slightly affected the 3D wedging angle (< 2°) and its location (< 4°) for the ID. As for the clinical evaluation, average angular errors were less than 0.4° in the radiographic frontal and lateral planes. The mean 3D wedged angles were about 4.9° ± 1.9° for the VB and 6.0° ± 1.7° for the ID. Linear relations were found between the 2D and the 3D angles, but the 3D angles were located on diagonal planes statistically different than the radiographic ones (between 100° and 221°). There was no statistical relation between the 2D radiographic angles and the locations of the 3D intervertebral wedging angles. These results clearly indicate that VB and ID endplates are wedged in 3D, and that measurements on plain radiographs allow incomplete evaluation of spinal wedging. Clinicians should be aware of these limitations while using wedging measurements from plain radiographs for diagnosis and/or research on scoliotic deformities.

Key words Scoliosis · Spinal wedging (vertebral wedging, discal wedging) · 3D reconstruction · Vertebral endplates · Spinal deformations · Projected angles

Introduction

Idiopathic scoliosis is a complex three-dimensional (3D) deformity of the spine and rib cage that involves intrinsic deformations of the vertebral bodies, the intervertebral disks, and the ribs. The spinal components are generally wedged, and the spine results in a complex 3D torsional S-shape curve [13, 16].

The literature reports few studies that document the scoliotic spinal wedging in the frontal and sagittal planes using clinical standard radiographs or cadaveric spine specimens [5–7, 12, 14, 15, 17, 20]. A 2D evaluation of the wedging phenomenon was usually made by using the projection of vertebral body corners (or a best-fitted line passing through each vertebral endplate) in the frontal or sagittal plane. In these studies, the angle between two consecutive projected endplates gives the 2D wedging angle in each of these planes. In the thoracic segment of moderate and severe scoliosis, the apical vertebrae appear to be wedged in such a way that the anterior part of the vertebral body is longer than the posterior part [5–7].

Three-dimensional CT was used by Kojima and Kurokawa [8] to quantify the deformities of scoliotic vertebral bodies, but the measured angles were computed from projections on vertebral frontal and sagittal planes. Only a few studies have tried to document the wedging phenomenon in other planes with a 3D perspective [10, 12, 14, 15]. These studies were mostly done on dry cadaveric adult specimens with severe scoliotic deformities using a vernier caliper instrument, a magnetic digitizer, or elective plane radiographs. Perdriolle et al. [14, 15] observed that the smallest vertebral body thickness is postero-lateral. They also noted that the wedging phenomenon was more closely related to the intervertebral disk deformation for mild scoliosis (Cobb angle < 30°) and tended to affect more equally the vertebral body and the intervertebral disk in severe scoliosis [12]. Two-dimensional observations obtained by Ronchetti et al. [17] in the radiographic frontal plane showed that as the scoliotic curves progress, the vertebrae become more wedged with respect to the disks.

All these studies contributed to understand the etiology and progression of scoliosis. However, in the clinical context of scoliosis management, it is obvious that the spinal projections on the 2D radiographic planes do not give a full and accurate interpretation of the complex 3D intrinsic deformities of the spine, and it is thought that 2D measurements could lead to a biased evaluation of scoliotic deformities. In other respects, published methods do not allow analysis in a routine clinical context of the individual intrinsic spinal deformities of scoliotic patients in a 3D perspective. This paper presents a method that was developed and validated to allow the 3D reconstruction of the contours of vertebral body endplates from two standard biplanar radiographs, and measurement of the 3D wedging angles regardless of vertebral position or orientation in space. This approach has been used to verify whether 2D radiographic measurements are adequate and do not lead to biased evaluations of spinal wedging.

Materials and methods

Reconstruction of vertebral endplates and measurement of spinal 3D wedging

The 3D reconstruction of vertebral endplates is based on a multi-view radiographic technique that has been detailed in previous publications [1, 3]. This method allows the 3D reconstruction of corresponding anatomical landmarks on two or more radiographs using a calibration object and the Direct Linear Transformation (DLT) algorithm [11]. It has been adapted for the particular reconstruction of vertebral body endplate contours of any vertebra. Most of this adapted approach has been presented in Dansereau et al. [4] and it is outlined in summary below:

1. Take standard PA and lateral radiographs of patients (or any spine segment) installed in a positioning apparatus containing a calibration object for 3D reconstruction with the DLT algorithm. This object is composed of two acrylic sheets in which are embedded 50 radiopaque steel balls of 2-mm diameter, whose 3D coordinates are known with an accuracy of 0.4 mm [3] (Fig. 1).
2. Digitize on both radiographs the vertebral body extremities (non-corresponding points) in addition to the calibration steel balls and six standard anatomical landmarks: the vertebral endplate centers and the tips of both pedicles on each vertebra (which are usually and routinely taken for the spinal reconstruction procedure [3]) (Fig. 1).
3. Calculate the 3D coordinates of the six standard anatomical landmarks using the DLT algorithm [3] (Fig. 1).
4. Calculate the axial rotation. To do so, a local coordinate system is first defined on each vertebra (the Z and Y axis are respectively constructed with the lines joining the vertebral body endplate centroids and the pedicle tips, while the X axis is obtained by the cross-product of Y and Z). Then, the axial rotation is calculated by interpreting the coefficients of the transformation matrix, which express the local coordinate system in relation to the global coordinate system (the latter is the one proposed by the Scoliosis Research Society [19], where X, Y, and Z are the anterior, left, and cephalad directions).
5. Project the digitized extremities of the vertebral body on planes parallel to the frontal and lateral radiographic planes, defined at the vertebral endplate center, and fit an ellipse through these points with respect to the calculated vertebral axial rotation (Fig. 2).
6. Retro-project the new computed extremities of this ellipse onto the frontal and lateral radiographic planes using in an inverse way the DLT equations, and correct the vertebral endplate center landmarks accordingly (Fig. 2).
7. Repeat steps 3 to 6 until convergence. The convergence criterion is based on the variation of position of the vertebral body center (which has to be inferior to 0.5 mm). Two or three iterations are normally needed to obtain convergence.

At the end of this 7-step procedure (named "3D reconstruction procedure"), the vertebral endplates are modeled as 3D-oriented ellipses in space and are dimensioned with adequate diameters.

Three-dimensional wedging angles of the vertebral bodies and intervertebral disks as well as their angular location were then computed by finding the location of the shortest and longest distances between two adjacent endplates along their contours (Fig. 3). The "3D wedging angle" represents the maximum angle between two consecutive vertebral endplate planes, and can be cal-

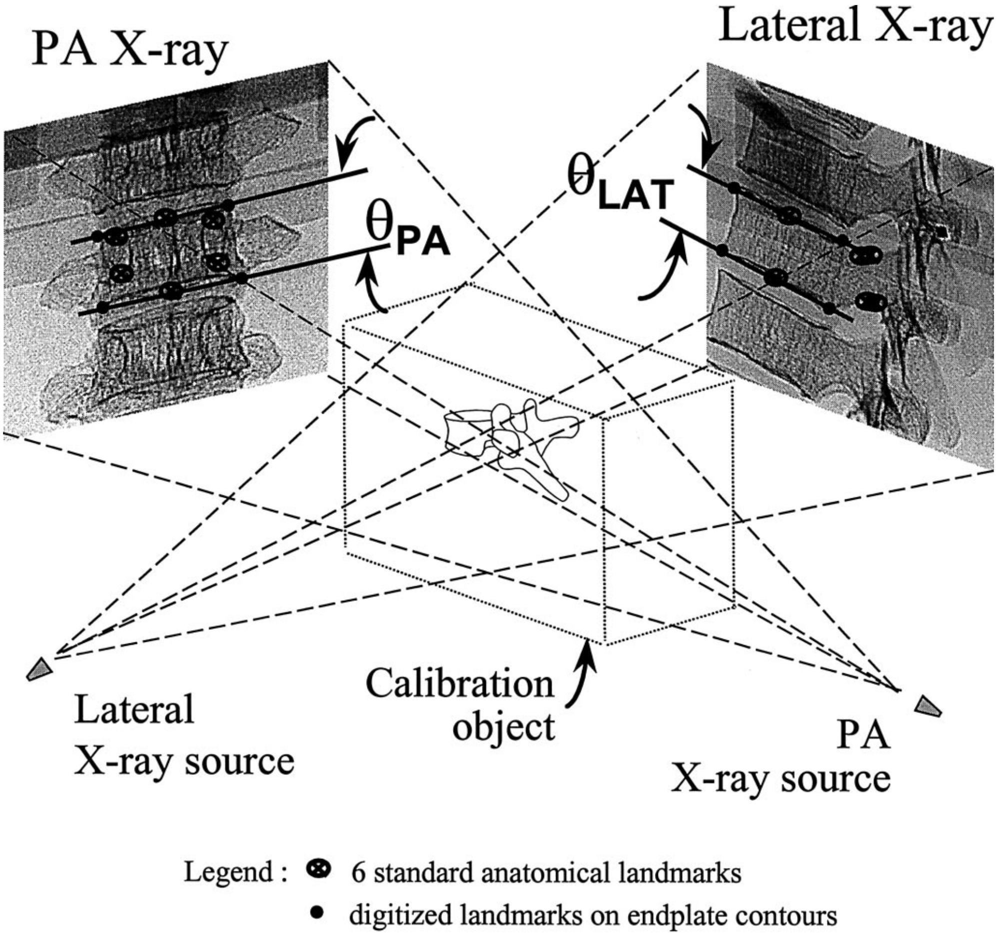

Fig. 1 Biplanar radiographic configuration with the anatomical landmarks (pedicle tips, vertebral endplate centers, and corners) identified on postero-anterior (PA) and lateral radiographs

culated either for the vertebral body or the intervertebral disk. The angular location of this maximum 3D wedging angle in space (Fig. 3) is given with respect to the *vertebral* frontal plane, i.e., the local plane *YZ* defined at step 4 of the 3D reconstruction procedure (or the superior adjacent vertebra in the case of the intervertebral disk). Two-dimensional wedging angles can also be calculated with the parallel projection of the reconstructed ellipses on vertebral frontal and sagittal planes (Fig. 3), or on the global frontal and sagittal radiographic planes (as defined by the Scoliosis Research Society and described at step 4) (Fig. 1).

Validation methods for the reconstruction and measurement techniques

The method for the 3D reconstruction of vertebral body endplates and the measurement of 3D wedging angles was evaluated with three different approaches: (1) an in-vitro comparison with precise measurements; (2) a mathematical sensitivity study to assess the influence of reconstruction errors; and (3) a clinical evaluation and comparison with standard 2D wedging angles.

In-vitro comparison with precise measurements

This first approach consisted of comparing the 3D modeled endplates of a functional unit (T_8-T_9) taken from a normal cadaveric spine (without evident wedging) to their precise 3D measurements obtained using a coordinate measuring machine (PH10M Probe Head mounted on a 3D digitizer G90C, LK Tool USA), the accuracy of which is close to 0.1 mm. The functional unit was mounted on a 3 degrees of freedom (3-DOF) apparatus, which allows the positioning of the vertebrae with different angles in space (Fig. 4). The centroid of T8 was approximately placed near the center of rotation of this apparatus. A 15° radio-transparent plastic quoin was introduced between the two vertebrae to simulate the intervertebral wedging. Eleven different vertebral angular positions that represent pure or combined rotations were individually given to the functional unit (Table 1). These angles represent possible or extreme spatial positions for scoliotic vertebrae. They were introduced using equivalent rotations about the global axis in a given sequence (R*z*, R*y*, and R*x*) to match the projected angles of Table 1 and to prevent 3D rotation errors [18]. At each position, PA and lateral X-rays were taken, and the endplates were reconstructed in 3D with the 3D reconstruction procedure. Using the coordinate measuring machine, the endplate contours were digitized (about 50 points for each endplate, at 2-mm intervals along the contour) as well as other points on pedicle tips and on the apparatus. The latter points were used to transform the measured coordinates in the same referential system as the reconstructions. The reconstructions were then compared with the 3D measurements by means of geometric parameters (vertebral body thickness, endplate plane orientation, wedging orientation, position of points on endplate contours) calculated with the data obtained by each method.

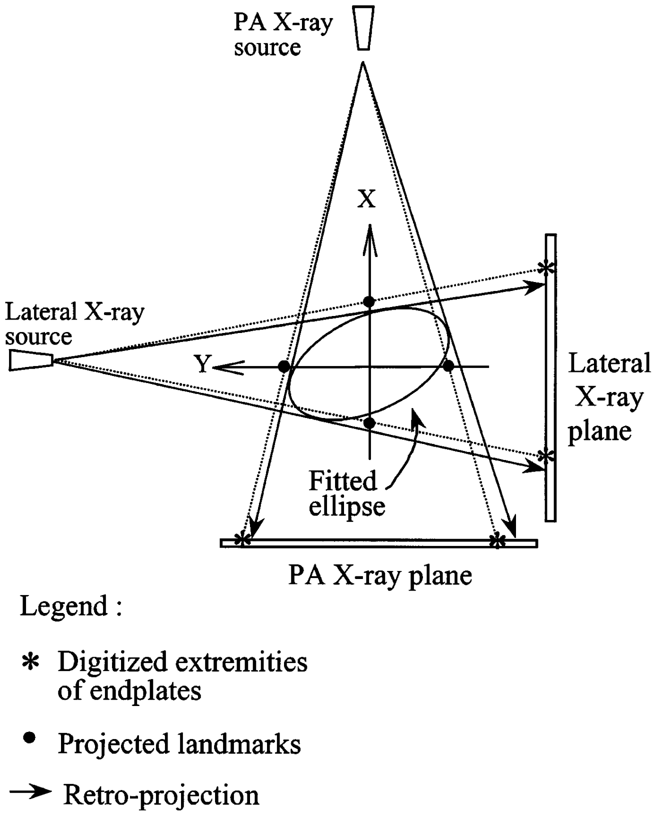

Fig. 2 Projection of endplate extremities on planes parallel to X-rays to generate an ellipse representing the endplate contours, and retro-projection of the new computed extremities of this ellipse on X-ray planes

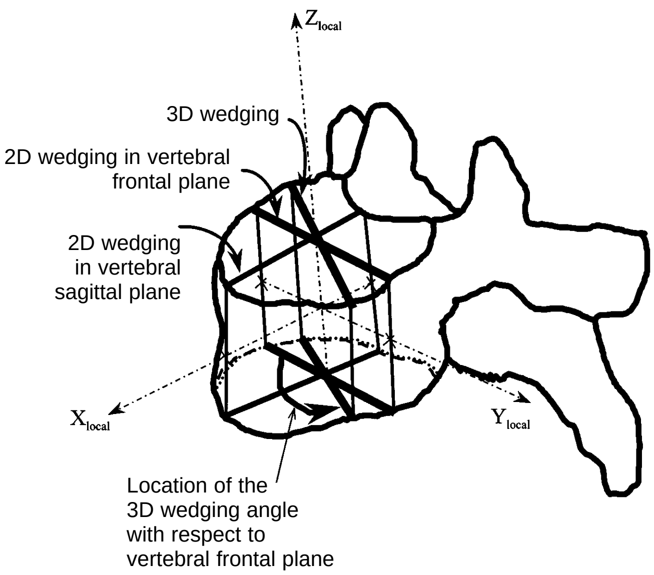

Fig. 3 Two-dimensional (2D) wedging angles in vertebral frontal and sagittal planes, as well as the maximum 3D wedging angle and its angular location

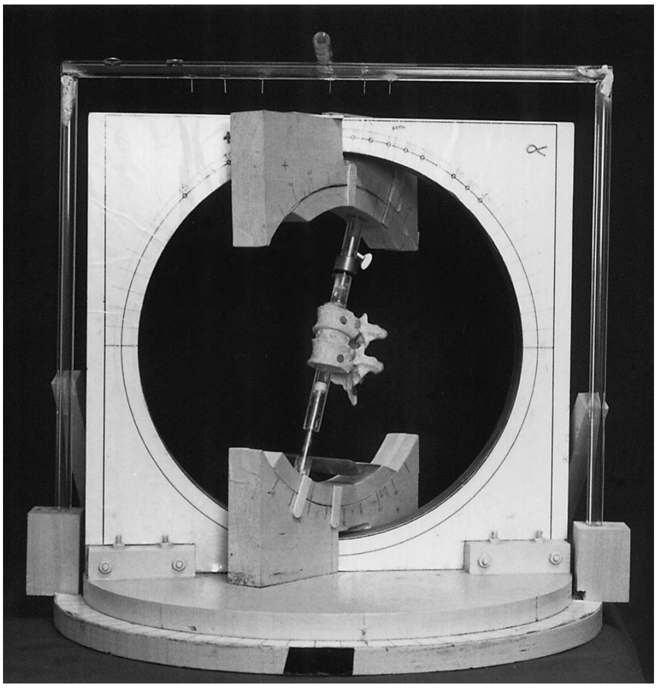

Fig. 4 Three degrees of freedom apparatus used for the positioning of the vertebrae with different angles in space

Table 1 Nominal angles (in degrees) given to the functional unit specimen for the in-vitro validation with precise measurements

Case no.	Axial rotation (Rz)	Frontal rotation (R*x*)	Sagittal rotation (R*y*)
1	0	0	0
2	–20	0	0
3	40	0	0
4	0	10	0
5	0	–30	0
6	0	0	10
7	0	0	–20
8	–20	10	0
9	–20	0	10
10	0	10	10
11	–20	10	10

Sensitivity study

This study was performed to assess the influence of digitizing errors on the reconstructions and on the computation of the 3D wedging angle and its location. Using the same normal functional unit (T_8-T_9 with the imposed 15° intervertebral wedging), different errors were randomly generated on the 2D coordinates of all digitized landmarks. These errors had a normal distribution (centered at 0 mm), and four different standard deviations (SD) were tested: 0.5, 1, 2, and 3 mm. These errors correspond to possible or maximum reconstruction errors that can be found for this reconstruction technique (cf. results from the first validation and Aubin et al. [2]). One hundred different functional units were mathematically generated for each value of SD. In each case, the endplates were reconstructed using the 3D reconstruction procedure, and the

3D wedging angles were calculated. For each SD value, the calculated wedging angles were compared with the original ones (without the introduced errors) and the differences were statistically analyzed using the average, the standard deviation, and the unpaired Student *t*-tests.

Clinical evaluation and comparisons of the 2D and 3D wedging angles

This third evaluation was done on 26 scoliotic patients presenting moderate right thoracic curves (Cobb angles between 25° and 45°, with a mean at 37°), and 8 patients with small thoracic Cobb angles (between 15° and 25°). The biplanar X-rays were taken during the scoliosis clinics at Sainte-Justine Hospital. The vertebral endplates of the two vertebrae located at the thoracic apical level (including the intervertebral disk) were reconstructed in 3D using the 3D reconstruction procedure. On both radiographs, the clinical wedging angles were measured and compared with the reconstructed angles projected on the frontal and sagittal planes. The maximum 3D wedging angles and their angular locations were then computed for each patient and also compared with the 2D angles using statistical tests.

Results

Figure 5 shows the resulting spinal reconstruction of a typical patient presenting a right thoracic and a left lumbar curve that can be obtained with the 3D reconstruction procedure. It can be seen that the vertebral endplates are modeled as 3D-oriented ellipses in space and are dimensioned with adequate and realistic diameters.

Mean errors (± SD) for the 11 angular positions of the two cadaveric vertebrae mounted on the 3-DOF positioning apparatus were:

1.7 ± 0.9 mm for the position of points on endplate contours

0.5 ± 0.4 mm for vertebral body thickness

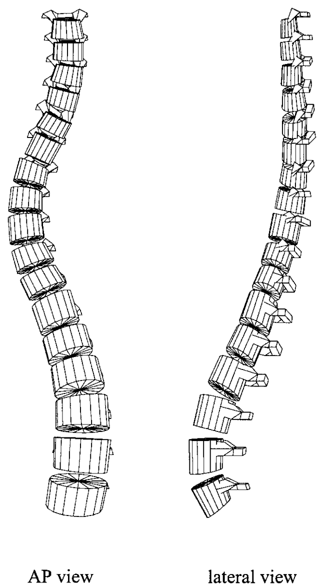

Fig. 5 Antero-posterior (AP) and lateral views of a typical scoliotic spine obtained with the endplate reconstruction technique

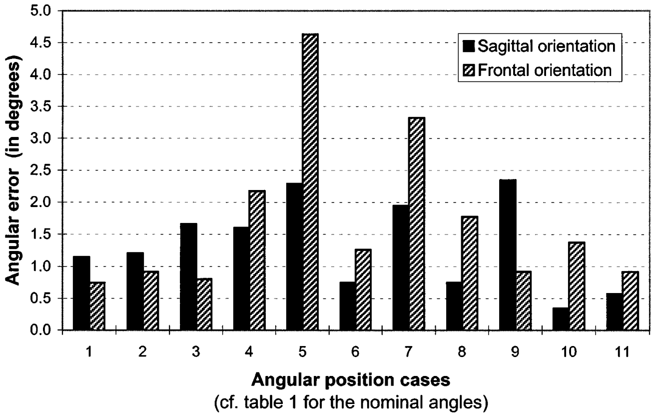

Fig. 6 Endplate orientation errors related to the position of points taken on endplate contours for the 11 different angular positions (cf. Table 1)

Table 2 Effect of introducing errors on the two-dimensional (2D) coordinates of the digitized landmarks (*SD* standard deviation)

Simulated errors on digitized landmarks (StD in mm)	Mean errors for the intervertebral disks	
	3D wedging angle	Wedging angle location
0.5	0.5° ± 0.4°	2.2° ± 1.6°
1.0	1.0° ± 0.8°	4.2° ± 3.3°
2.0	1.9° ± 1.5°	3.8° ± 5.7°
3.0	3.2° ± 2.6°	11.1° ± 9.1°

1.3° ± 0.7° for endplate plane sagittal orientation (around the local *Y* axis)

1.7° ± 1.2° for endplate plane frontal orientation (around the local *X* axis)

2.2° ± 1.4° for endplate plane 3D orientation

11° ± 6° for the *location* of the 3D wedging angle (about 3 mm along the endplate contour)

The greatest errors occurred when the cadaveric functional unit was oriented with frontal or sagittal rotation angles superior to 20° (cases 5 and 7, Fig. 6). The errors on the endplate plane 3D orientation are reduced to 1.7° ± 0.8° when these extreme and infrequent vertebral frontal and sagittal rotations superior to 20° are excluded. In other respects, the orientation errors were quite independent of the axial rotation for any angle combination or vertebral spatial position.

As for the sensitivity study, errors inferior to 2 mm on the digitization of anatomical landmarks affected slightly the 3D wedging measurements on the 3D reconstructed endplates of the intervertebral disk (less then 2° for the wedging angle and less than 4° for its location; Table 2). The vertebral body 3D wedging angle errors (not shown in Table 2) were found to be quite similar to those found

Table 3 Wedging of the vertebral bodies and intervertebral disks at the thoracic apical level

	2D wedging angles				Maximum 3D wedging angles	
	Radiographic planes		Intrinsic vertebral planes			
	Frontal	Sagittal	Frontal	Sagittal	Angle	Location[a]
Vertebral bodies	4.1° ± 1.9°	2.0° ± 1.5°	4.2° ± 1.8°	2.0° ± 1.4°	4.9° ± 1.9°	167° ± 23°
Intervertebral disks	4.9° ± 1.7°	2.0° ± 1.6°	5.1° ± 1.8°	1.7° ± 1.4°	6.0° ± 1.7°	170° ± 18°

[a] With respect to the vertebral frontal plane

for the intervertebral disk. However, in this particular case, the endplates were nearly parallel, and when digitizing errors superior to 2 mm were introduced, the computer method became unstable. Nevertheless, even in this case, the wedging measurement errors were quite small (< 0.2° for the 2D wedging angles), as found in the group of eight patients with mild scoliosis.

As for the clinical evaluation on the thoracic apical functional units of 26 scoliotic patients, average errors were less than 0.4° in frontal and lateral radiographic planes. The maximum 3D wedging angles were statistically greater than the 2D angles measured on radiographs. Linear relations were found between the 2D angles measured on radiographs and the maximum 3D wedging angles (for the vertebral bodies: r = 0.92 in frontal plane, r = 0.55 in sagittal plane; for the intervertebral disks: r = 0.83 in frontal plane, r = 0.32 in sagittal plane). However, the maximum 3D angles were located on diagonal planes statistically different than the intrinsic frontal and sagittal planes of the vertebrae (for the vertebral bodies: 167° ± 23°, min 100°, max 211°; for the intervertebral disks: 170° ± 18°, min 142°, max 221°, with respect to the vertebral frontal plane). There was no linear relation between the 2D radiographic angles and the locations of the 3D intervertebral wedging angles.

Discussion and conclusions

The method presented in this paper allows the evaluation in a clinical routine context of the intrinsic 3D scoliotic vertebral body and intervertebral disk wedging. Validation results showed that this approach is fairly accurate for the reconstruction of vertebral endplates and can allow efficient measurement of the maximum 3D wedging angles of vertebral endplates. However, the measurement of the maximum 3D wedging angles and their location may be altered when the endplates are nearly parallel (very small wedging angles), because the maximum and minimum distances between adjacent endplates tend to be equal. In particular, this measurement was found to be affected by infrequent digitization errors superior to 2 mm. In reality, the wedging measurement errors were quite small, as found for the eight patients with the smallest Cobb angles. Moreover, in the sensitivity study that was performed using a normal functional unit (without evident vertebral body deformation), the errors on the location of the maximum wedging were relatively small (< 4° for digitization errors of 2 mm, which corresponds to an error of less than 2 mm on the identification of the location of the maximum wedging site along the vertebral endplate contour). Based on the validation results, it can be assumed that the reconstruction technique could be rightly used to evaluate intrinsic vertebral and intervertebral changes within the evolution of scoliotic spinal deformities.

This is one of the first studies that considers the scoliotic wedging as a truly 3D-oriented angle in space and that uses a method which could be utilized routinely in a clinical context, in contrast to the CT-scan approach of Kojima and Kurokawa [8]. This approach reveals in a 3D way how the scoliotic spine is intrinsically deformed and could also indicate how the scoliotic spine transformations will occur. It also shows that the projection of the wedged spine on the 2D radiographic planes does not allow a full and accurate interpretation of the complex 3D wedging of the vertebral bodies and intervertebral disks.

The clinical results clearly indicate that vertebral and intervertebral wedging in thoracic scoliosis are not 2D deformations but a 3D phenomenon because maximum wedging values at the apex do not occur in a plane parallel to the frontal or sagittal plane, but are oriented obliquely in a 3D way in space. The large dispersion of results indicates that the maximum 3D wedging angles at the apex are scattered and occur in planes other than the frontal one. These results are consistent with the geometrical shape of the scoliotic curves, but do not completely agree with published observations and reported values of Perdriolle et al. [12, 14] for the general location of the maximum 3D wedging angle. This can be explained by the fact that Perdriolle's specimens had very severe lordoscoliosis curves as opposed to the moderate hypokyphotic scoliosis curves included in this study. It was not possible to reach conclusions for the eight patients with mild scoliosis because of the small number of subjects. However, similar trends to the ones of the group of 26 patients with moderate scoliosis were found.

The linear relations between the 2D wedging angles evaluated on radiographic planes and real 3D wedging angles indicate that measurements on radiographs give reliable information that allows partial characterization of the vertebral body wedging. However, radiographic measurements lead to an incomplete evaluation of the intrinsic scoliotic 3D wedging of the vertebral bodies and of the intervertebral disks. In addition, the location of the maximum wedging angle can not be obtained nor deduced from radiographic measurements. Clinicians should be aware of these limitations while using wedging measurements from radiographs for diagnosis and/or research on scoliotic deformities.

Using this validated approach, more clinical evaluations can be made to gain a full understanding of the 3D wedging phenomenon and its relation to the spinal complex torsional deformities in space. The method presented in this paper may help clinicians and researchers in their attempt to study the development of scoliotic deformities during the clinical course of scoliosis, and to correlate etiology and/or treatment with the scoliotic vertebral endplate wedging phenomenon.

Acknowledgements Research funded by the Natural Sciences and Engineering Research Council of Canada and the "Projet Défi" program (Canada). Special thanks to Maxime Roy for the digitization of the X-rays.

References

1. André B, Dansereau J, Labelle H (1994) Optimized vertical stereobase radiographic setup for the clinical 3-D reconstruction of the human spine. J Biomech 8: 1023–1035
2. Aubin C-É , Dansereau J, Parent F, Labelle H, de Guise JA (1997) Morphometric evaluations of personalized 3-D reconstructions and geometric models of the human spine. Med Biol Eng Comput 35 : 611–618
3. Dansereau J, Beauchamp A, de Guise JA, Labelle H (1990) Three-dimensional reconstruction of the spine and the rib cage from stereoradiographic and imaging techniques. Proceedings of the 16th Conference of the Canadian Society of Mechanical Engineering, Toronto, Canada, vol 2, pp 61–64
4. Dansereau J, Chabot A, Huynh NT, Labelle H, de Guise JA (1995) 3-D reconstruction of vertebral endplate wedging. Three-dimensional Anal Spinal Deform 15: 69–73
5. Deacon P, Flood BM, Dickson RA (1984) Idiopathic scoliosis in three dimensions. A radiographic and morphometric analysis. J Bone Joint Surg [Br] 66: 509–512
6. Deane G, Duthie RB (1973) A new projectional look at articulated scoliosis spines. Acta Orthop Scand 44: 351–365
7. Dickson RA, Lawton JO, Archer IA, Butt WP (1984) The pathogenesis of idiopathic scoliosis. Biplanar spinal asymmetry. J Bone Joint Surg [Br]66: 8–15
8. Kojima T, Kurokawa T (1992) Quantification of three-dimensional deformity of idiopathic scoliosis. Spine 17: S22–S29
9. Labelle H, Dansereau J, Bellefleur C, Jéquier JC (1995) Variability of geometric measurements from three-dimensional reconstructions of scoliotic spines and rib cages. Eur Spine J 4: 88–94
10. LeBorgne P, Skalli W, Stokes IAF, Maurel N, Duval-Beaupère G, Lavaste F (1995) Three-dimensional measurement of a scoliotic spine. Three-dimensional Anal Spinal Deform 15: 219–224
11. Marzan GT (1976) Rational design for close-range photogrammetry. Thesis, University of Illinois at Urbana-Champaign
12. Perdriolle R (1979) La scoliose: son étude tridimensionnelle. Maloine, Paris
13. Perdriolle R, Vidal J (1985) Thoracic idiopathic scoliosis curve evolution and prognosis. Spine 10: 785–791
14. Perdriolle R, Becchetti S, Vidal J, Lopez P, Maury P (1992) Description de la cunéiformisation de la vertèbre apicale. Proceedings of the First International Symposium on 3-D Scoliotic Deformities, Éditions de l'École Polytechnique de Montréal and Gustav Fisher Verlag, Montréal, pp 244–249
15. Perdriolle R, Becchetti S, Vidal J, Lopez P (1993) Mechanical process and growth cartilages – essential factors in the progression of scoliosis. Spine 18: 343–349
16. Poncet P, Dansereau J, Labelle H (1995) Elimination of numerical instability on smoothed scoliotic spinal curves. Three-dimensional Anal Spinal Deform 15: 127–132
17. Ronchetti PJ, Stokes IAF, Aronsson DD (1997) Vertebral body and disc wedging in scoliosis. Research into spinal deformities I, studies in health technology and informatics, vol 37. IOS Press, pp 81–84
18. Skalli W, Lavaste F, Descrimes J-L (1995) Quantification of three-dimensional vertebral rotations in scoliosis – what are the true values? Spine 20: 546–553
19. Stokes IAF (1994) Three-dimensional terminology of spinal deformity. Spine 19: 236–248
20. Xiong B, Sevastik JA, Hedlung R, Sevastik B (1994) Radiographic changes at the coronal plane in early scoliosis. Spine 19: 159–164